

1 **CO<sub>2</sub>-wettability of low to high rank coal seams: Implications for carbon sequestration**  
2 **and enhanced methane recovery**

3  
4 Muhammad Arif <sup>a,b,\*</sup>, Ahmed Barifcani <sup>a</sup>, Maxim Lebedev <sup>a</sup>, Stefan Iglauer <sup>a</sup>

5  
6 <sup>a</sup> Curtin University, Department of Petroleum Engineering, 26 Dick Perry Avenue, 6151  
7 Kensington, Australia

8 <sup>b</sup> University of Engineering and Technology, Lahore 54890, Pakistan

9  
10  
11 **Abstract**

12 Coal seams offer tremendous potential for carbon geo-sequestration with the dual benefit of  
13 enhanced methane recovery. In this context, it is essential to characterize the wettability of  
14 the coal-CO<sub>2</sub>-water system as it significantly impacts CO<sub>2</sub> storage capacity and methane  
15 recovery efficiency. Technically, wettability is influenced by reservoir pressure, coal seam  
16 temperature, water salinity and coal rank. Thus a comprehensive investigation of the impact  
17 of the aforementioned parameters on CO<sub>2</sub>-wettability is crucial in terms of storage site  
18 selection and predicting the injectivity behaviour and associated fluid dynamics. To  
19 accomplish this, we measured advancing and receding water contact angles using the pendent  
20 drop tilted plate technique for coals of low, medium and high ranks as a function of pressure,  
21 temperature and salinity and systematically investigated the associated trends. We found that  
22 high rank coals are strongly CO<sub>2</sub>-wet, medium rank coals are weakly CO<sub>2</sub>-wet, and low rank  
23 coals are intermediate-wet at typical storage conditions. Further, we found that CO<sub>2</sub>-  
24 wettability of coal increased with pressure and salinity and decreased with temperature  
25 irrespective of coal rank. We conclude that at a given reservoir pressure, high rank coal  
26 seams existing at low temperature are potentially more efficient with respect to CO<sub>2</sub>-storage  
27 and enhanced methane recovery due to increased CO<sub>2</sub>-wettability and thus increased  
28 adsorption trapping.

## 30 1. Introduction

31 Carbon capture and storage (CCS) is the most promising approach to mitigate anthropogenic  
32 CO<sub>2</sub> emissions and thus ensure a cleaner environment [1-5]. The storage of CO<sub>2</sub> in depleted  
33 oil and gas reservoirs [6-8] or deep saline aquifers [9-11] allows trapping of enormous  
34 volumes over a long period of time. Another option is injection of CO<sub>2</sub> into coal seams [12-  
35 15] with the dual benefit of enhanced coal bed methane recovery [16-18]. In conventional  
36 reservoirs, CO<sub>2</sub> is held trapped by means of four mechanisms which are structural trapping  
37 [19-22], capillary or residual trapping [8,23-25], dissolution trapping [26,27] and mineral  
38 trapping [28]. In coal seams, however, the dominant storage mechanism is adsorption  
39 trapping of CO<sub>2</sub> onto the coal matrix [12,29,30]. Typically the adsorption capacity of CO<sub>2</sub> is  
40 higher than that of methane, depending on coal rank [31-33]; consequently, CO<sub>2</sub> displaces  
41 methane towards the production well and itself gets sorbed within the micropores of the coal  
42 seam and remains trapped. The preferential adsorption and thus storage of CO<sub>2</sub> in coal seams,  
43 by forced migration of methane, is strongly influenced by wettability of the CO<sub>2</sub>-water-coal  
44 system [12,34], which in turn is generally a function of reservoir pressure [34-37],  
45 temperature and salinity. Moreover, in coal seams wettability is also a function of coal rank,  
46 vitrinite reflectance, fixed carbon and ash content [35,38]. Therefore, it is essential to  
47 describe CO<sub>2</sub>-wettability of coals of varying ranks, and how reservoir conditions (pressure,  
48 temperature and brine salinity) influences this wettability.

49 In this context, several studies reported CO<sub>2</sub>-wettability of coals at ambient conditions [38-  
50 41], but only a limited amount of literature data for the more relevant higher pressures have  
51 been reported [34-37,42,43]. Table 1 presents a summary of the major experimental variables  
52 considered in previous studies, and this work.

53

54

55

56

57 Table 1: CO<sub>2</sub>-wettability of coals: Summary of experimental conditions used.

58

Reference	Pressure	Temperature	Salinity	Coal type	Overall Coal rank
Chi et al. [42]	up to 6.2 MPa	298K	DI water	Not mentioned	Not mentioned

Siemons et al. [37]	up to 14 MPa	318K	DI water	Anthracite	High
Sakurovs and Lavrencic, [36]	up to 15 MPa	313 K	DI water	Bituminous	Medium
Kaveh et al. [43]	up to 16 MPa	318K	DI water	High volatile bituminous	Medium
Kaveh et al. [35]	up to 16 MPa	318K	DI water	Semi anthracite, High volatile bituminous	High and Medium
Saghafi et al. [34]	up to 6 MPa	295K	DI water	Medium volatile bituminous	Medium
This study	up to 20 MPa	308K, 323K and 343K	0wt% - 10wt% NaCl	Semi-anthracite, Medium volatile bituminous, Lignite	High, Medium and Low

59

60

61 Therefore there is a clear lack of data available on CO<sub>2</sub>-wettability of coals as a function of  
62 coal rank, coal formation pressure, and particularly temperature and salinity (cp. Table 1).  
63 Thus there exists a gap in terms of proper understanding of CO<sub>2</sub>-wettability of coal seams of  
64 different ranks at reservoir conditions. Moreover, although it is well established that coal  
65 seams offer enormous potential for enhanced methane recovery and CO<sub>2</sub> sequestration, yet  
66 certain important questions need to be addressed which are: 1) Which type of coal (low rank,  
67 medium rank, or high rank) are most suitable for CO<sub>2</sub> storage and enhanced coalbed methane  
68 recovery under the prevailing geothermal and reservoir pressure conditions? 2) Is the  
69 suitability of CO<sub>2</sub> sequestration in coal seams of a particular rank valid for a wide range of  
70 reservoir pressures, temperatures and salinity conditions? 3) What mechanisms are  
71 responsible for long term CO<sub>2</sub>-storage in coals? To answer these questions and to generally  
72 improve the characterization of CO<sub>2</sub>-wettability of coals, we experimentally measured water  
73 advancing and receding contact angles on three coal samples as a function of coal rank (low,  
74 medium and high ranks), vitrinite reflectance and fixed carbon at different CO<sub>2</sub> pressures (0.1  
75 MPa to 20 MPa), temperatures (ranging from 308K to 343K), and brine salinities (0wt%  
76 NaCl-10wt% NaCl) using the pendent drop technique. The results of the study lead to a broad  
77 characterization of CO<sub>2</sub>-wettability of coals and thus help optimize CO<sub>2</sub>-storage and  
78 enhanced coal bed methane recovery operations. Our results indicate that CO<sub>2</sub>-wettability of

79 coals is strongly influenced by coal rank such that the high rank coals are more CO<sub>2</sub>-wet and  
80 low rank coals are least CO<sub>2</sub>-wet at a given reservoir pressure, temperature and salinity.

81

82

## 83 **2. Materials and methods**

84

### 85 *2.1. Coal Samples*

86 Three coal samples [high rank (semi anthracite; from Hazelton, Pennsylvania, USA), medium  
87 rank (medium volatile bituminous; from Morgantown, West Virginia, USA), and low rank  
88 (lignite; from North Dakota, USA; Table 2)] were used in this research. The samples were cut  
89 to cuboid shape (~1cm x 1cm x 0.5cm) and the surface roughness of each substrate was  
90 measured with an atomic force microscope (AFM instrument model DSE 95-200); note that  
91 surface roughness significantly affects contact angle measurements [44,45]. The RMS surface  
92 roughness of the specific coal substrates used were 840nm, 880nm and 280nm for high,  
93 medium and low rank coals respectively.

94

### 95 *2.2. Petrology, Ultimate and Proximate Analysis*

96 The results of the proximate, ultimate and petrological analysis and the internal properties  
97 (density and volume) of the coal samples are listed in Table 2. Note that coal samples of  
98 different rank differ mainly in volatile matter, moisture, fixed carbon and vitrinite reflectance  
99 [46,47]. Petrology was analysed in accordance with Australian Standard AS2856 and  
100 ISO7404; proximate analysis were conducted using AS1038.3, ISO11722 and ASTM D3172-  
101 07a, and ultimate analysis were performed using AS1038.6 and ISO 609.

102

103

104

105

106 **Table 2.** Properties of coal samples used.

Sample	Rank	Semi-Anthracite	Medium-volatile Bituminous	Lignite
	Geological Location		Hazelton,	Morgantown,

		Pennsylvania	West Virginia	
	Overall rank (used in this work)	High rank	Medium rank	Low rank
Petrology	Vitrinite Reflectance ( $R_r$ , % <sup>*</sup> )	3.92	0.82	0.35
	Vitrinite (%)	89.6	73.1	83
	Liptinite (%)	0	3.4	4
	Inertinite (%)	7.6	18.8	10.8
	Minerals (%)	2.8	4.7	2.1
Proximate analysis	Moisture (air dried, %)	2.6	2	16.3
	Ash (%)	9.7	6.4	7.8
	Volatile Matter (%)	2.9	32.4	34.8
	Fixed carbon (%)	84.9	59.2	41.1
Ultimate analysis	Ash (%)	9.7	6.4	7.8
	Carbon (%)	82.6	78.6	54.6
	Total Hydrogen (%)	2.35	5.07	5.27
	Hydrogen (%)	2.06	4.85	3.45
	Nitrogen (%)	1.16	1.54	0.62
	Total Sulphur (%)	0.8	0.99	0.66
	Oxygen by difference (%)	3.68	7.62	2.87
Properties	Bulk density (g/cc)	1.30	1.28	1.44
	Dry sample volume (cc)	16.55	12.77	4.26
	Dry mass (g)	21.17	16.194	6.159
	RMS Surface Roughness (nm)	840	880	280

\* All percentages in above table represent weight percent

107

108

### 109 2.3. Fluids

110

111 99.9 wt% CO<sub>2</sub> (from BOC, gas code – 082), de-ionized water (Conductivity: 0.02 mS/cm),  
 112 and 5wt% and 10wt% NaCl brine (NaCl Source: Scharlab s.l., Spain, Purity: ≥0.995mass%)  
 113 were used in the study. Acetone (99.9 wt%) was used to wash the coal samples.

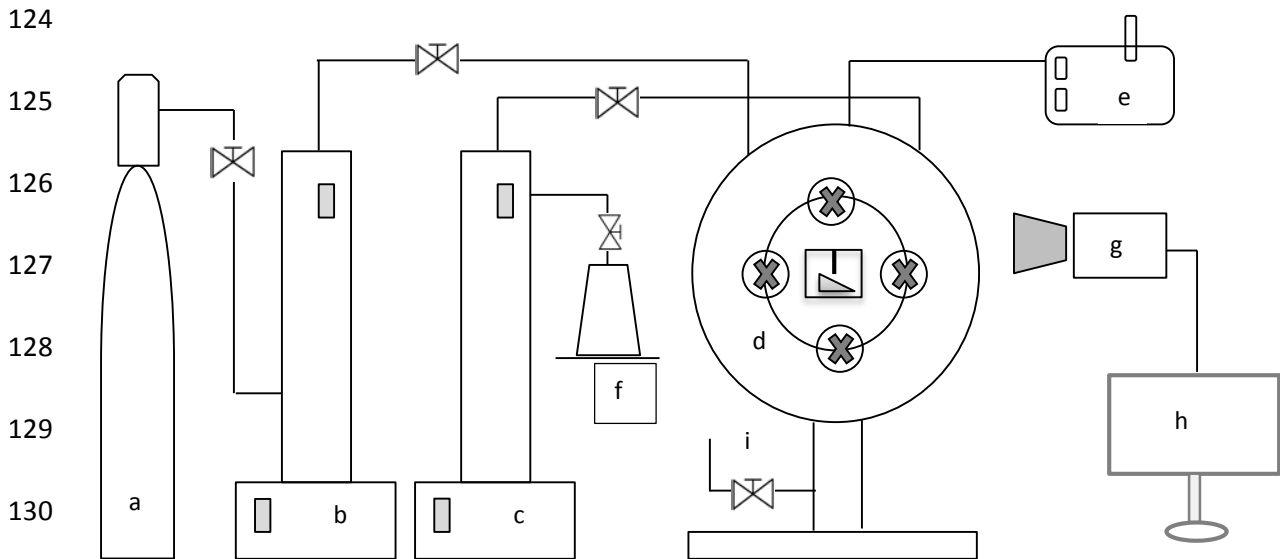
114

115

### 116 2.3. Contact angle measurements

117 CO<sub>2</sub>-brine wettability was measured using the pendent drop tilted plate technique [48]. The  
 118 experimental setup is shown in Figure 1; it consists of a high pressure cell (which holds the

119 sample on a tilted plate), a CO<sub>2</sub> cylinder, two high precision syringe pumps (Teledyne D-500,  
120 pressure accuracy of 0.1%FS) for water and CO<sub>2</sub> and a video camera. Prior to each  
121 experiment, the coal substrates were washed with acetone and then cleaned in air plasma  
122 (Diemer Yocto instrument) for 2 minutes to ensure that no organic contaminants are  
123 deposited on the sample, which would introduce a bias [49].



133 **Figure 1.** Experimental setup for contact angle measurements used in this study; (a) CO<sub>2</sub>  
134 cylinder (b) high precision syringe pump-CO<sub>2</sub>, (c) high precision syringe pump-water, (d)  
135 high pressure cell with substrate housed on a tilted plate inside, (e) heating unit, (f) liquid  
136 feed/drain system, (g) high resolution video camera, (h) image visualization and  
137 interpretation software, (i) pressure relief valve.

139 For each measurement, a clean and dry coal sample was placed inside the pressure cell onto  
140 the tilted plate. The temperature was set to a fixed value (308K, 323K, and 343K), and CO<sub>2</sub>  
141 pressure in the cell was increased with a high precision syringe pump to pre-determined  
142 values (0.1 MPa, 5 MPa, 10 MPa, 15 MPa, 20 MPa) by injecting CO<sub>2</sub> into the cell.  
143 Subsequently a droplet of de-gassed brine (average volume of  $\sim 6\mu\text{L} \pm 1\mu\text{L}$ ) was allowed to  
144 flow (at 0.4ml/min) and was dispensed onto the substrate through a needle. We note that the  
145 fluids used were not thermodynamically equilibrated, since earlier studies demonstrated that  
146 the contact angle  $\theta$  is not significantly affected by mass transfer during the first 60seconds of

147 exposure (only insignificant change ( $2^\circ$ ) was observed by [50,51]) and during this time all  
148 measurements were completed. Furthermore, non-equilibrated fluids are most relevant at the  
149 leading edge of the CO<sub>2</sub> plume, i.e. when CO<sub>2</sub> first encounters under saturated brine. A video  
150 camera (Basler scA 640–70 fm, pixel size = 7.4  $\mu\text{m}$ ; frame rate = 71 fps; Fujinon CCTV lens:  
151 HF35HA-1B; 1:1.6/35 mm) recorded the entire process, and contact angles were measured on  
152 images extracted from the movie files. Advancing ( $\theta_a$ ) and receding water contact angles ( $\theta_r$ )  
153 were measured simultaneously at the leading and trailing edges of the droplet, just before the  
154 droplet started to move. The standard deviation of these measurements was  $\pm 3^\circ$  based on  
155 replicate measurements; however for lignite the standard deviation reached  $\pm 5^\circ$ , which is due  
156 to the more complicated nature of the sample.

157

158

### 159 **3. Results and Discussion**

160 In order to assess CO<sub>2</sub>-storage and methane recovery potential, CO<sub>2</sub>-wettability of coals was  
161 characterized as a function of rank at relevant thermophysical conditions by measuring  
162 advancing and receding contact angles on coal samples of high, medium and low ranks at  
163 various reservoir conditions (pressure range: 0.1-20 MPa, temperature range: 308K-323K and  
164 salinity range: 0wt%-10wt% NaCl). The outcomes of the study led to a precise realisation of  
165 the relationships between coal rank and corresponding CO<sub>2</sub> geo-storage and ECBM potential.  
166 The subsequent sections describe the results in detail.

167

#### 168 *3.1. Effect of Pressure on CO<sub>2</sub>-wettability of coal*

169 The effect of pressure was systematically tested on the three (high, medium, low rank)  
170 samples at 0.1 MPa, 5 MPa, 10 MPa, 15 MPa and 20 MPa for three different temperatures  
171 (308K, 323K, and 343K). Both,  $\theta_a$  and  $\theta_r$ , clearly increased with pressure at all temperatures  
172 for all coal samples (Figure 2-4). High rank coal was water wet ( $\theta < 50^\circ$ , [21]) at ambient  
173 pressure for all temperatures tested (308K-343K; Figure 2). As pressure increased from 0.1  
174 MPa to 20 MPa at 323K,  $\theta_a$  increased from  $51^\circ$  to  $141^\circ$  and  $\theta_r$  increased from  $45^\circ$  to  $129^\circ$  (red  
175 lines in Figure 2), and thus high rank coal became CO<sub>2</sub>-wet at high pressure ( $\theta > 130^\circ$ , [21]).  
176 Similarly, at 343K, as pressure increased from ambient to 20 MPa,  $\theta_a$  increased from  $58^\circ$  to  
177  $118^\circ$  and  $\theta_r$  increased from  $52^\circ$  to  $107^\circ$ .

178 This increase in contact angle with pressure is consistent with independent experimental data  
179 on coal [34-37,42,43,52]. Specifically, Chi et al. [42] measured contact angles up to 6.2 MPa

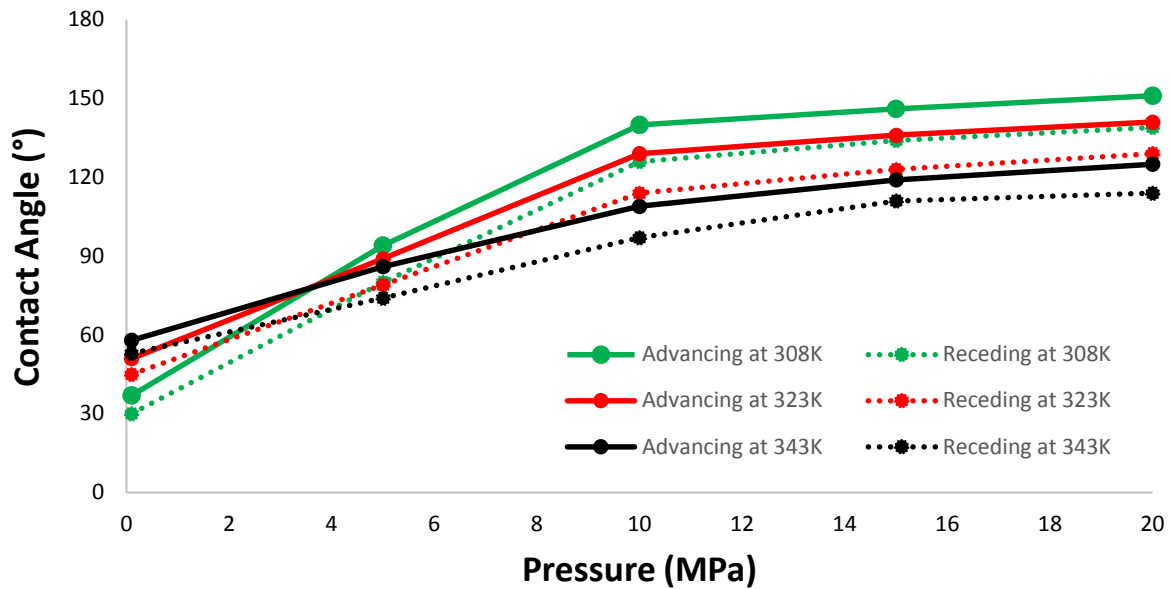
180 at 298K for coals of unknown ranks and found that coal hydrophobicity increased with  
181 pressure. Siemons et al. [37] extended the testing pressure up to 14 MPa at 318K and  
182 analysed CO<sub>2</sub>-water contact angle for an anthracite coal (high rank) and found that the system  
183 became CO<sub>2</sub>-wet at 2.6 bar, however, in our case semi-anthracite became weakly CO<sub>2</sub>-wet at  
184 around 7 MPa ( $\theta_a > 110^\circ$ ); this difference could be due to difference in rank of the samples  
185 (semi-anthracite in this study) and difference in experimental conditions (temperature and  
186 surface cleaning methods). Sakurovs and Lavrencic [36] experimentally determined CO<sub>2</sub>-  
187 water contact angles using the captive bubble technique up to 15 MPa at 313K for low to  
188 medium rank coals ( $R_v\%$  of their samples ranged from 0.62-1.4) and found an increase in  
189 CO<sub>2</sub>-wettability with pressure for all samples. Kaveh et al. [35] compared CO<sub>2</sub>-wettability of  
190 high volatile bituminous (medium rank) and semi anthracite (high rank) coals up to 16 MPa  
191 and at 318K; and reported that semi-anthracite became CO<sub>2</sub>-wet ( $\theta = 110^\circ$ ) at 5.7 MPa which  
192 is close to our result (7 MPa); the slight difference could be due to different surface cleaning  
193 methods and temperature. Saghafi et al. [34] also studied CO<sub>2</sub>-wettability of high rank coal  
194 up to 6 MPa at 295K, their sample turned CO<sub>2</sub>-wet at 5 MPa ( $\theta = 110^\circ$ ).

195 The increase in contact angle with pressure is also consistent with experimental data on pure  
196 minerals such as mica [53-56] and quartz [50,51,55,57]. This transformation of wettability  
197 from water-wet to CO<sub>2</sub>-wet by an increase in pressure is, apart from increased intermolecular  
198 interactions of CO<sub>2</sub> with solid surface [53,58], also related to the increased adsorption of CO<sub>2</sub>  
199 on the coal surface, which is evident from experimental CO<sub>2</sub> adsorption data on coals [33,59-  
200 62].

201

202 Since adsorption is the dominant storage mechanism in coals, and typically accounts for 98%  
203 of the total gas stored [12,63], high pressure storage conditions are preferred as they would  
204 lead to increased storage volumes. Moreover, increased CO<sub>2</sub>-wettability of coal will lead to  
205 more uniform distribution of CO<sub>2</sub> within the micropores of the coal seams and thus improved  
206 displacement of methane towards the production wells. However, at high pressures coal  
207 swells [64-66], which leads to a significant permeability decrease [67], which again limits the  
208 Darcy flow (of the CO<sub>2</sub>) and thus injectivity.





210

211 **Figure 2.** CO<sub>2</sub>-DI water contact angles on high rank coal (semi-anthracite) at tested  
 212 pressures (0.1 MPa-20 MPa) and temperatures (308K-343K).

213

214 Furthermore, we found that the rate of contact angle increase with pressure is sharper for the  
 215 pressure range 0.1 MPa-10 MPa (Figure 2). For example, at 323K,  $\theta_a$  measured 51° at 0.1  
 216 MPa and 129° at 10 MPa resulting in a net increase of 78°, whereas the net increase in  $\theta_a$  for  
 217 the pressure range 10 MPa-20 MPa was only 12°. This implies that injection of CO<sub>2</sub> in high  
 218 rank coals at very high pressure may yield only marginal benefits in terms of additional  
 219 volume stored because of only marginal improvement in CO<sub>2</sub>-wettability. Generally, the  
 220 increase in contact angle with pressure flattened out for pressures 10 MPa-20 MPa.

221

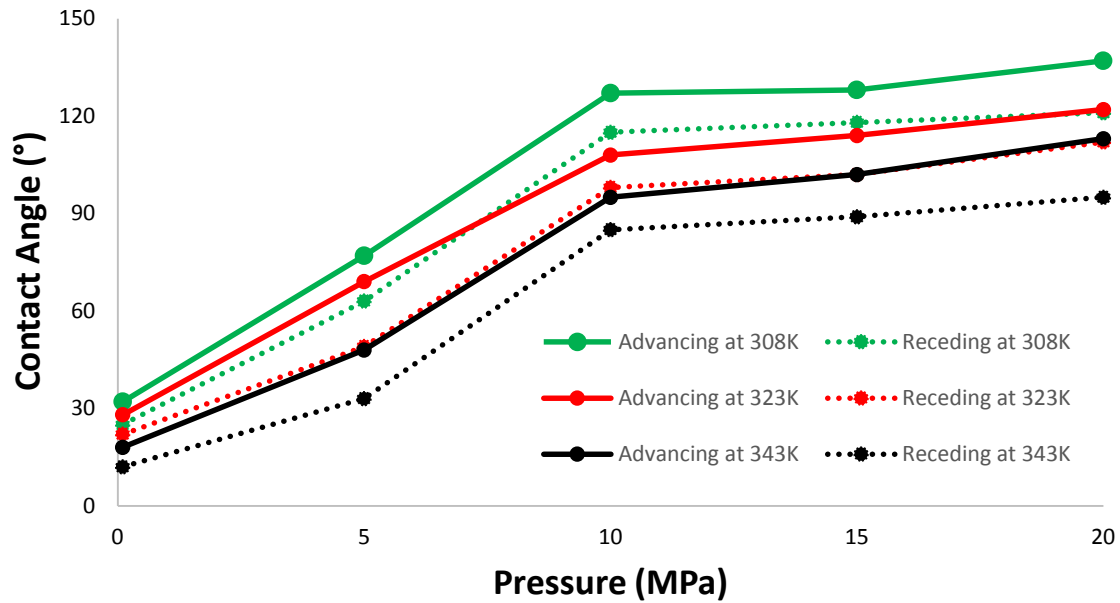


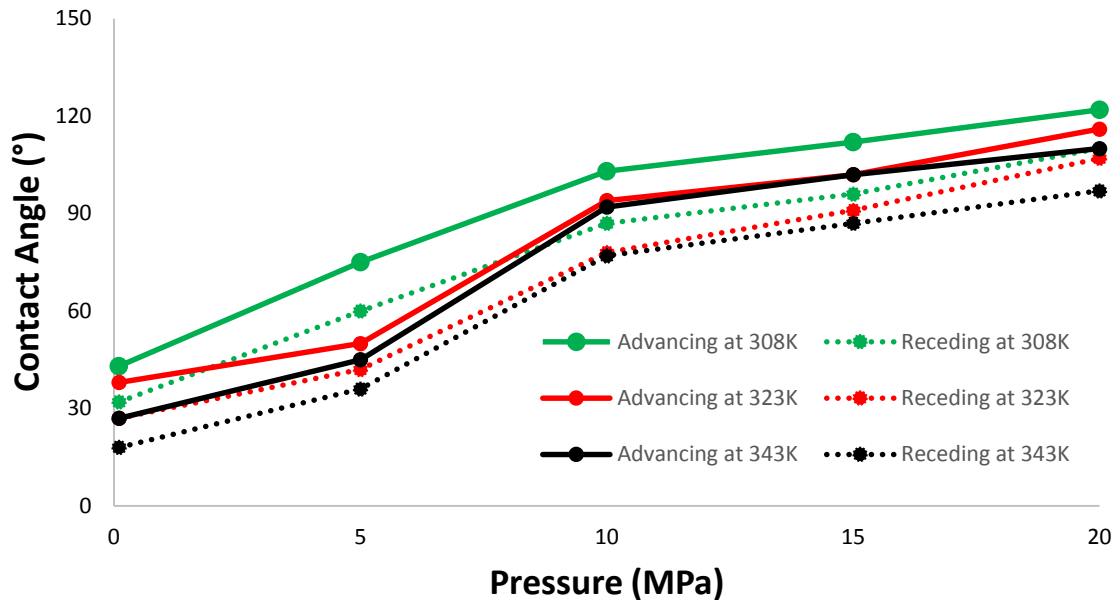
**Figure 3.** CO<sub>2</sub>-DI water contact angles on medium rank coal (medium volatile bituminous) at tested pressures (0.1 MPa-20 MPa) and temperatures (308K-343K).

The medium rank coal sample (medium volatile bituminous coal) remained water-wet (at ambient conditions) with a maximum  $\theta_a$  value of 32° (Figure 3). When pressure increased from 0.1 MPa to 20 MPa at 323K,  $\theta_a$  increased from 28° to 122° and  $\theta_r$  increased from 18° to 113°. Consequently, the system, which was water-wet at ambient conditions, turned weakly CO<sub>2</sub>-wet at reservoir conditions ( $110^\circ \leq \theta \leq 130^\circ$ ; [21]). Likewise high rank coal, the increase in contact angle for medium rank coal was sharp up to 10 MPa; however, the increase gradually flattened (between 10-20 MPa). The results, therefore, imply that CO<sub>2</sub> storage capacity in medium rank coals increases with pressure at all temperatures owing to the increased CO<sub>2</sub>-wetting which implies to increased adsorption trapping; however, this storage capacity increase is only marginal at higher pressures, e.g. from 15 MPa to 20 MPa. Therefore, from an economic standpoint, for practical storage purposes an optimal injection pressure must be selected.

For low rank coals, contact angles increased with pressure at all temperatures as shown in Figure 4. For example, at 308K, a sharp increase was observed for pressure 0.1 MPa to 10 MPa, and the curve flattened afterwards. However, at 323K, the change in contact angle with pressure followed a slightly inconsistent trend such that contact angles first increased gradually up to 5 MPa ( $\theta_a$  increased from 38° to 50° when pressure increased from 0.1 MPa to 5 MPa), then sharply up to 10 MPa ( $\theta_a$  measured from 92°), and then a small increase was

245 observed up to 20 MPa ( $\theta_a$  increased to  $116^\circ$ ). The maximum contact angle measured for low  
 246 rank coals was  $122^\circ$  (at 20 MPa and 308K) indicating that the most hydrophobic wettability  
 247 regime for low rank coals is ‘weakly CO<sub>2</sub>-wet’ implying reduced CO<sub>2</sub> trapping by means of  
 248 adsorption. Similar trends were observed for higher temperature (323K and 343K).

249



250

251 **Figure 4.** CO<sub>2</sub>-DI water contact angles on low rank coal (lignite) at tested pressures (0.1  
 252 MPa-20 MPa) and temperatures (308K-343K).

253

254

### 255 3.2. Effect of temperature on CO<sub>2</sub>-wettability of coal

256

257 The trends of contact angle variation with temperature are presented in Figures 2-4. For all  
 258 coal samples analysed, both,  $\theta_a$  and  $\theta_r$ , decreased with temperature at all pressures tested, with  
 259 the exception that for high rank coal,  $\theta_a$  and  $\theta_r$  increased with temperature at ambient pressure  
 260 (0.1 MPa). For example, when temperature increased from 308K to 343K at 0.1 MPa,  $\theta_a$   
 261 increased from  $37^\circ$  to  $58^\circ$  for high rank coal, while it decreased from  $32^\circ$  to  $18^\circ$  for medium  
 262 rank coal and from  $43^\circ$  to  $27^\circ$  for low rank coal. At higher pressures (5 MPa-20 MPa),  
 263 however, all coal types showed a clear decrease in  $\theta_a$  and  $\theta_r$  with temperature (Figures 2-4).  
 264 For simplicity a summary of contact angle variation with temperature is shown in Figure 5.  
 265 At 15 MPa, for high rank coal, when temperature increased from 308K to 323K,  $\theta_a$  decreased  
 266 from  $146^\circ$  to  $119^\circ$ , implying wettability transformation from strongly CO<sub>2</sub>-wet to weakly  
 267 CO<sub>2</sub>-wet. Similarly, for medium rank coal,  $\theta_a$  decreased from  $128^\circ$  to  $102^\circ$  when temperature

268 increased from 308K to 343K. However, for low rank coal,  $\theta_a$  first decreased from 112° to  
 269 102° when temperature increased from 308K to 323K, and then became constant when  
 270 temperature increased further (from 323K to 343K). In summary, CO<sub>2</sub>-wettability of coal  
 271 decreased with increasing temperature irrespective of the coal rank. There is no published  
 272 data on the effect of temperature on CO<sub>2</sub>-water-coal contact angles, however, the decrease in  
 273 contact angle with temperature has also been reported for pure minerals such as mica [53,54]  
 274 or quartz [56-58].

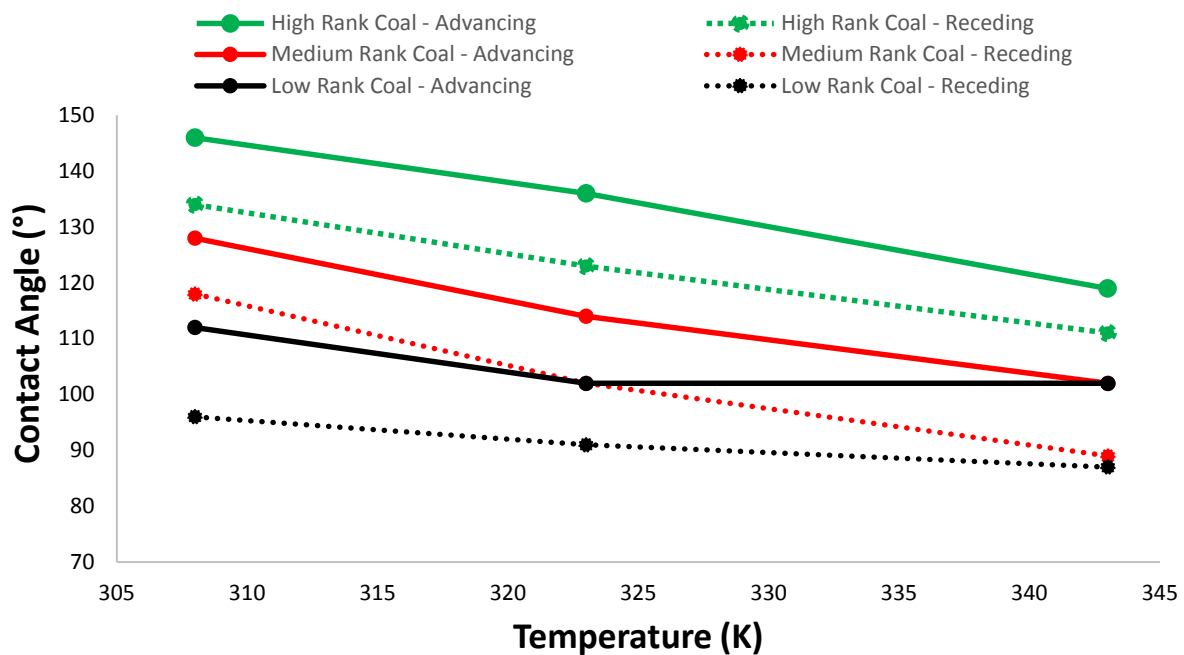
275

276 We demonstrate that two distinct mechanisms may be held responsible for the decrease in  
 277 contact angle with temperature. The first mechanism is the interplay of the three interfacial  
 278 tensions [53,58], which is expressed by the Young-Laplace equation as follows:

$$279 \quad \cos\theta = \frac{\gamma_{sv} - \gamma_{sl}}{\gamma_{vl}} \quad (1)$$

280 In eq. (1),  $\gamma_{sv}$  and  $\gamma_{sl}$  are the solid-CO<sub>2</sub> interfacial tension and solid-brine interfacial tension,  
 281 respectively, whereas  $\gamma_{vl}$  is CO<sub>2</sub>-brine interfacial tension. Since most of the previous studies  
 282 [51,53,57,68] agree that CO<sub>2</sub>-brine interfacial tension increases with temperature, it is evident  
 283 from equation (1) that the difference of solid-CO<sub>2</sub> interfacial tension and solid-brine  
 284 interfacial tension (numerator of equation) should increase with temperature to cause a  
 285 corresponding decrease in contact angle with temperature.

286



287

288

289 **Figure 5.** Effect of temperature on CO<sub>2</sub>-wettability for all coal samples used in the study.  
290 For simplicity measurements are shown only for 15 MPa.

291

292 Secondly, the decrease in the contact angle with temperature can be attributed to the CO<sub>2</sub>  
293 adsorption behaviour on coal. The experimental studies on the effect of temperature on CO<sub>2</sub>  
294 adsorption [69-74] report that there is a clear decrease in CO<sub>2</sub> adsorption on coal surfaces  
295 with temperature. This reduced CO<sub>2</sub>-affinity is thus reflected in the contact angles. Perera et  
296 al. [71] mentioned that the decrease in adsorption capacity with temperature is due to the  
297 increase in kinetic energy and rate of diffusion of CO<sub>2</sub>, which tend to release gas molecules  
298 from the coal matrix resulting in a corresponding reduction in net amount of adsorbed gas.  
299 We thus conclude that low temperature coal seams have higher CO<sub>2</sub> storage capacities in  
300 comparison to high temperature coal seams.

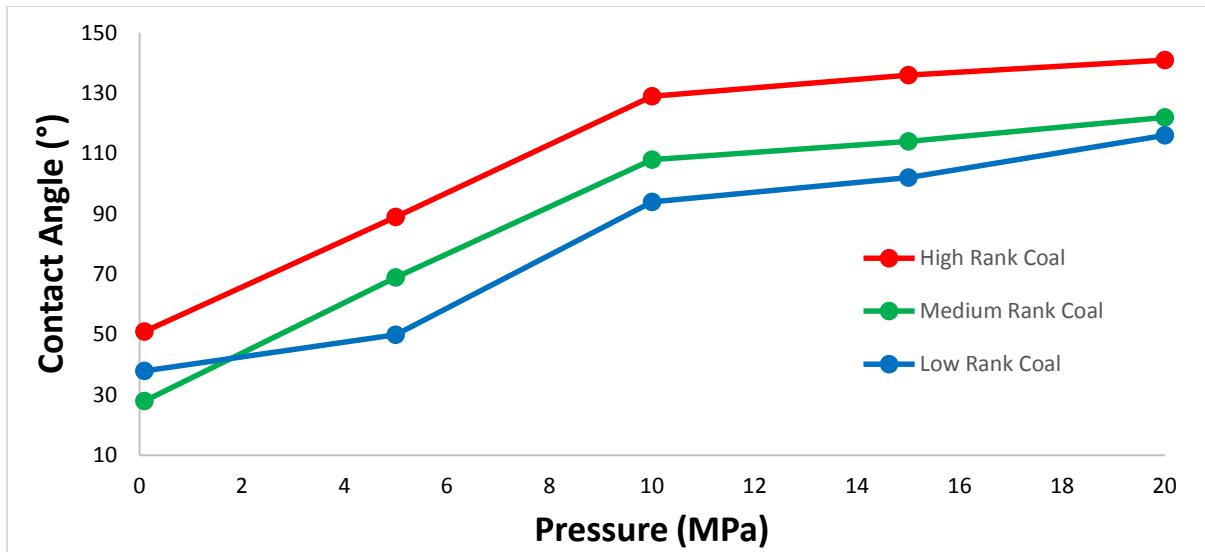
301

### 302 3.3. *Effect of coal rank on CO<sub>2</sub>-wettability*

303

304 In order to demonstrate the impact of coal rank on CO<sub>2</sub>-wettability and thus on methane  
305 production and CO<sub>2</sub> storage potential in coals, we plotted advancing water contact angles  
306 (only for simplicity) as a function of pressure and temperature (Figure 6). It is clear that at  
307 any given CO<sub>2</sub> pressure, apart from the ambient, high rank coal offers highest CO<sub>2</sub>-wetting  
308 potential, and CO<sub>2</sub>-wettability substantially decreases with rank. Low rank coals (e.g.  
309 Lignite) are least CO<sub>2</sub>-wet and medium rank coal (e.g. Bituminous) are intermediate. These  
310 results are in agreement with Kaveh et al. [35] who compared CO<sub>2</sub>-wettability of semi-  
311 anthracite and high volatile bituminous coals, and they measured higher contact angles for  
312 semi-anthracite coals, and thus they concluded that hydrophobicity of coals increases with  
313 coal rank. Moreover, Sakurovs and Lavrencic [36] also concluded that high ranks coals were  
314 easier to wet with CO<sub>2</sub> at high pressures and that the increase in CO<sub>2</sub>-wettability promoted  
315 the rate of penetration of CO<sub>2</sub> into the coals. It can therefore be established that CO<sub>2</sub>-  
316 wettability of coals is a strong function of coal rank and that high rank coals are more CO<sub>2</sub>-  
317 wet. We point out that this behaviour is related to the increase in CO<sub>2</sub> adsorption capacity  
318 with an increase in coal rank as evidenced by the literature data on adsorption isotherms of  
319 coals of varying rank [32,75].

320



322

323 **Figure 6.** Effect of coal rank on CO<sub>2</sub>-wettability.

324

325

326 *3.4. Effect of brine salinity on CO<sub>2</sub>-wettability of coal*

327

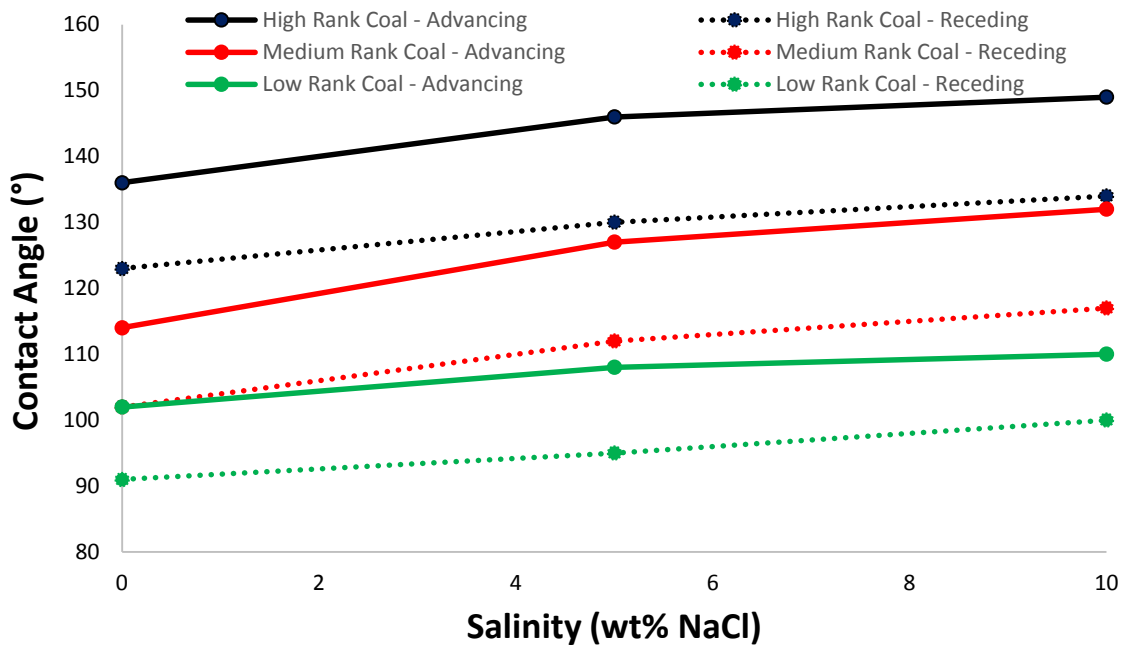
328 Water can exist in coals seams in the form of free water in cleats, chemically bound hydration  
 329 water, and water adsorbed onto the surface of the matrix blocks [76,77]. The cleat system is  
 330 initially filled with water and it provides the flow path for production by Darcy's law. We  
 331 thus analysed the impact of brine salinity on CO<sub>2</sub>-brine-coal wettability for various salinities  
 332 (0wt% NaCl, 5wt%NaCl and 10wt% NaCl) at 15 MPa and 323K on all the coal samples  
 333 studied in this work; as salinity is expected to vary in subsurface coal seams [78].

334 Both,  $\theta_a$  and  $\theta_r$ , increased with salinity for all coal samples (Figure 7). This increase was  
 335 stronger for the brine salinity increase from 0wt% NaCl to 5wt% NaCl; e.g. for medium rank  
 336 coal,  $\theta_a$  increased from 114° to 127° and  $\theta_r$  increased from 102° to 112° when salinity  
 337 increased from 0wt% NaCl to 5wt% NaCl brine. For the salinity increase from 5wt% NaCl to  
 338 10wt% NaCl, the increase in contact angle was very small; e.g. for medium rank coal,  $\theta_a$   
 339 increased from 127° to 132° and  $\theta_r$  increased from 112° to 116° when salinity increased from  
 340 5wt% NaCl to 10wt% NaCl brine. Moreover, we found similar trends for low, medium and  
 341 high rank coals (Figure 7). In the literature, there is a lack of data on the effect of salinity on  
 342 CO<sub>2</sub>-wettability of coal, yet our results are consistent with Ibrahim et al. [52], who analysed  
 343 contact angles of CO<sub>2</sub>-brine-coal systems for brine salinities varying between 0 g/L-15 g/L  
 344 NaCl), and who reported that contact angles were highest for 15 g/L and lowest for DI water.

345 Brine salinity thus does not exhibit major influence on contact angles at typical reservoir  
346 conditions.

347

348



349

350 **Figure 7.** Effect of salinity on CO<sub>2</sub>-wettability of coals at 323K and 15 MPa.

351

352

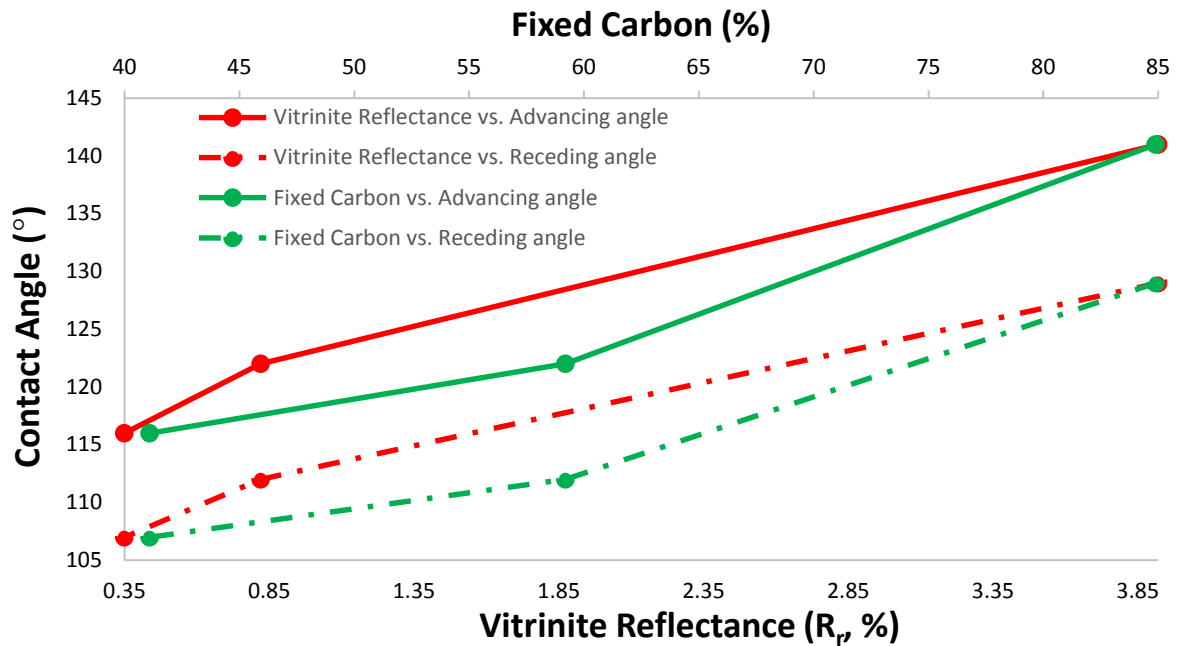
### 353 3.5. Relation between vitrinite reflectance, fixed carbon and coal wettability

354

355 There is a strong positive correlation between vitrinite reflectance and water contact angle.  
356 Similarly, fixed carbon (which is the solid combustible residue that remains after coal is  
357 heated and volatile matter is expelled) strongly correlates with the water contact angle  
358 (Figure 8). Practically, coals with higher vitrinite reflectance are more CO<sub>2</sub>-wet and thus will  
359 store more CO<sub>2</sub> by means of adsorption; coals with higher fixed carbon content also have  
360 better CO<sub>2</sub>-wetting characteristics. At 20 MPa and 323K, coal with a vitrinite reflectance ( $R_r$ ,  
361 %) of 3.8 is strongly CO<sub>2</sub>-wet ( $\theta_a = 140^\circ$ ), whereas at the same reservoir conditions medium  
362 rank coal ( $R_r = 0.82$ ) is weakly CO<sub>2</sub>-wet ( $\theta_a = 122^\circ$ ) and low rank coal ( $R_r = 0.35$ ) is  
363 intermediate-wet ( $\theta_a = 116^\circ$ ); thus CO<sub>2</sub> injection into low rank coals will require higher  
364 injection pressures to completely wet the surface in comparison to medium and high rank  
365 coals. Thus we conclude that coals of higher vitrinite reflectance and fixed carbon exhibit  
366 better CO<sub>2</sub> adsorption storage capacity, because of their better CO<sub>2</sub>-wettability. This effect

367 can be attributed to the non-polar nature of vitrinite matter which promotes de-wetting of the  
368 surface.

369



370

371 **Figure 8.** Variation of CO<sub>2</sub>-wettability with vitrinite reflectance and fixed carbon content.

372

#### 373 4. Implications

374

375 We measured CO<sub>2</sub>-wettability of coals of varying ranks; which is essential to assess the CO<sub>2</sub>  
376 storage potential of coal seams, and also to assess enhanced hydrocarbon gas production from  
377 unmineable coal seams. The measured data implies that CO<sub>2</sub> storage in coal seams is strongly  
378 influenced by pressure, seam temperature, brine salinity, rank of the coal, vitrinite reflectance  
379 and fixed carbon. As an example, consider three potential candidate coal bed methane  
380 formations of different ranks (high, medium and low) at a depth of 1km and at temperature of  
381 323K. The required CO<sub>2</sub> injection pressure will be approximately 10 MPa (estimated using  
382 formation pressure gradient ~ 10 MPa/km). We note that at 10 MPa and 323K, the values of  
383 the receding water contact angles for high, medium and low rank coals are 114°, 95° and 77°,  
384 respectively, implying that high rank coal is weakly CO<sub>2</sub>-wet, medium rank coal is  
385 intermediate-wet and low rank coal is weakly water-wet at storage conditions (note:  $\theta_r$  is  
386 considered here owing to the advancement of the CO<sub>2</sub> phase, which displaces brine; or  
387 alternatively ‘drainage’, Broseta et al. [54]). Consequently, the adsorption trapping capacities  
388 will be higher for high rank coal seams and least for low rank coal. Thus high rank coal will



389 be more suitable for CO<sub>2</sub> storage considering that adsorption of CO<sub>2</sub> is the dominant trapping  
390 mechanism [12,63]. Moreover, CO<sub>2</sub> injection into high rank coal at 10 MPa and 323K will  
391 wet the surfaces of coal with CO<sub>2</sub> better as compared to medium and low rank coals.  
392 Consequently, CO<sub>2</sub> will be distributed more uniformly into the micropores and thus recovery  
393 efficiency of methane will improve. It is also important to mention that with the increase in  
394 pressure and thus CO<sub>2</sub>-wettability, coal will swell inducing a permeability reduction [64-66]  
395 and this effect limits CO<sub>2</sub> storage in coal seams.

396

397 In summary, once injected, CO<sub>2</sub> will occupy the smallest pores (micropores of coal matrix)  
398 and brine will occupy larger pores (cleats), and as a result brine will be watered-out. In  
399 addition, it is experimentally proven that methane wettability of coal is lower than that of  
400 CO<sub>2</sub> [34], and the sorption capacities of CO<sub>2</sub> relative to CH<sub>4</sub> on the coal surface are 1.1 – 9.1  
401 times higher depending upon the coal rank [31,79-81]. Thus methane, which was adsorbed on  
402 the coal surfaces, will be displaced rather easily by CO<sub>2</sub>.

403

404

## 405 **5. Conclusions**

406

407 We measured water contact angles to characterize CO<sub>2</sub>-wettability of coals of low, medium  
408 and high rank as a function of reservoir pressure (0.1 MPa - 20MPa), temperature (308K-  
409 343K) and brine salinity (0wt% - 20wt%NaCl). The results demonstrate that both,  $\theta_a$  and  $\theta_r$ ,  
410 increase with pressure, consistent with [34-37] and the increase is quite rapid up to 10 MPa  
411 and it flattens if pressure is increased further (10 MPa-20MPa, Figure 2-4), implying that  
412 injection pressures must be optimized to ensure economic feasibility. The increase in contact  
413 angles with pressure is attributed to a) increased CO<sub>2</sub>-mineral intermolecular interactions due  
414 to increased CO<sub>2</sub> density [53,58], and b) increased CO<sub>2</sub> adsorption at high pressures [33,59-  
415 62]. Further we found that  $\theta_a$  and  $\theta_r$  decrease with temperature which is consistent with  
416 independent experimental CO<sub>2</sub>-adsorption data [69-74]. The influence of salinity was not  
417 significant, and  $\theta_a$  and  $\theta_r$  increased only slightly with elevated salt content. Moreover, and  
418 importantly, the CO<sub>2</sub>-wettability increased with the increase in coal rank, which is in  
419 agreement with other studies [35,36]. Specifically, we found that high rank coals (e.g. semi-  
420 anthracite) are strongly CO<sub>2</sub>-wet at typical storage conditions, while medium rank coals (e.g.  
421 medium volatile bituminous) are weakly CO<sub>2</sub>-wet and low rank coals (e.g. Lignite) are  
422 intermediate wet, i.e. CO<sub>2</sub>-wettability showed a positive correlation with vitrinite reflectance

423 and fixed carbon content. Finally, we predict that high rank coal seams existing at high  
424 temperatures and high pressures are more feasible for CO<sub>2</sub> storage due to increased CO<sub>2</sub>-  
425 wettability.

426

427

## 428 **Acknowledgements**

429

430 Energy Minerals (Queensland/Australia) is acknowledged for the proximate and ultimate  
431 analysis and Coal and Organic Services provider (NSW/Australia) is acknowledged for  
432 performing the coal petrology measurements. CSIRO (Western Australia) is acknowledged  
433 for the estimation of internal properties of the coal samples.

434

435

## 436 **References**

437

438 [1] Blunt, M., Fayers, F. J., & Orr, F. M. (1993). Carbon dioxide in enhanced oil  
439 recovery. *Energy Conversion and Management*, 34(9), 1197-1204.

440

441 [2] Iglauer, S., Paluszny, A., & Blunt, M. J. (2013). Simultaneous oil recovery and  
442 residual gas storage: A pore-level analysis using in situ X-ray micro-  
443 tomography. *Fuel*, 103, 905-914.

444

445 [3] Lackner, K. S. (2003). A guide to CO<sub>2</sub> sequestration. *Science*, 300(5626),  
446 1677.

447

448 [4] Metz, B., Davidson, O., de Coninck, H., Loos, M., & Meyer, L. (2005).  
449 *Carbon dioxide capture and storage*.

450

451 [5] Pentland, C. H., El-Maghraby, R., Iglauer, S., & Blunt, M. J. (2011).  
452 Measurements of the capillary trapping of super-critical carbon dioxide in  
453 Berea sandstone. *Geophysical Research Letters*, 38(6).

454

455 [6] Arts, R. J., Vandeweyer, V. P., Hofstee, C., Pluymaekers, M. P. D., Loeve, D.,  
456 Kopp, A., & Plug, W. J. (2012). The feasibility of CO<sub>2</sub> storage in the depleted

- 457 P18-4 gas field offshore the Netherlands (the ROAD project). *International*  
458 *Journal of Greenhouse Gas Control*, 11, S10-S20.
- 459
- 460 [7] Herzog, H., Drake, E., & Adams, E. (1997). CO<sub>2</sub> capture, reuse, and storage  
461 technologies for mitigating global climate change. *A White Paper*.
- 462
- 463 [8] Iglauer, S., Paluszny, A., Pentland, C. H., & Blunt, M. J. (2011a). Residual  
464 CO<sub>2</sub> imaged with X-ray micro-tomography. *Geophysical Research Letters*,  
465 38(21).
- 466
- 467 [9] André, L., Azaroual, M., & Menjoz, A. (2010). Numerical simulations of the  
468 thermal impact of supercritical CO<sub>2</sub> injection on chemical reactivity in a  
469 carbonate saline reservoir. *Transport in Porous Media*, 82(1), 247-274.
- 470
- 471 [10] Burton, M., Kumar, N., & Bryant, S. L. (2009). CO<sub>2</sub> injectivity into brine  
472 aquifers: Why relative permeability matters as much as absolute permeability.  
473 *Energy Procedia*, 1(1), 3091-3098.
- 474
- 475 [11] Dawson, G. K. W., Pearce, J. K., Biddle, D., & Golding, S. D. (2015).  
476 Experimental mineral dissolution in Berea Sandstone reacted with CO<sub>2</sub> or  
477 SO<sub>2</sub>-CO<sub>2</sub> in NaCl brine under CO<sub>2</sub> sequestration conditions. *Chemical*  
478 *Geology*, 399, 87-97.
- 479
- 480 [12] Gray, I. (1987). Reservoir engineering in coal seams: Part 1-The physical  
481 process of gas storage and movement in coal seams. *SPE Reservoir*  
482 *Engineering*, 2(01), 28-34.
- 483
- 484 [13] Lokhorst, A., & Wildenborg, T. (2005). Introduction on CO<sub>2</sub> Geological  
485 storage-classification of storage options. *Oil & Gas Science and*  
486 *Technology*, 60(3), 513-515.
- 487
- 488 [14] van Bergen, F., Krzystolik, P., van Wageningen, N., Pagnier, H., Jura, B.,  
489 Skiba, J., ... & Kobiela, Z. (2009). Production of gas from coal seams in the

- 490 Upper Silesian Coal Basin in Poland in the post-injection period of an ECBM  
491 pilot site. *International Journal of Coal Geology*, 77(1), 175-187.
- 492
- 493 [15] Mazzotti, M., Pini, R., & Storti, G. (2009). Enhanced coalbed methane  
494 recovery. *The Journal of Supercritical Fluids*, 47(3), 619-627.
- 495
- 496 [16] Busch, A., & Gensterblum, Y. (2011). CBM and CO<sub>2</sub>-ECBM related sorption  
497 processes in coal: a review. *International Journal of Coal Geology*, 87(2), 49-  
498 71.
- 499
- 500 [17] Damen, K., Faaij, A., van Bergen, F., Gale, J., & Lysen, E. (2005).  
501 Identification of early opportunities for CO<sub>2</sub> sequestration—worldwide  
502 screening for CO<sub>2</sub>-EOR and CO<sub>2</sub>-ECBM projects. *Energy*, 30(10), 1931-  
503 1952.
- 504
- 505 [18] Sams, W. N., Bromhal, G., Jikich, S., Ertekin, T., & Smith, D. H. (2005).  
506 Field- project designs for carbon dioxide sequestration and enhanced coalbed  
507 methane production. *Energy & Fuels*, 19(6), 2287-2297.
- 508
- 509 [19] Hesse, M. A., Orr, F. M., & Tchelepi, H. A. (2008). Gravity currents with  
510 residual trapping. *Journal of Fluid Mechanics*, 611, 35-60.
- 511
- 512 [20] Ketzer, J. M., Iglesias, R. S., & Einloft, S. (2012). Reducing Greenhouse Gas  
513 Emissions with CO<sub>2</sub> Capture and Geological Storage. In *Handbook of Climate  
514 Change Mitigation* (pp. 1405-1440). Springer US.
- 515
- 516 [21] Iglauer, S., Pentland, C. H., & Busch, A. (2015a). CO<sub>2</sub> wettability of seal and  
517 reservoir rocks and the implications for carbon geo-sequestration. *Water  
518 Resources Research*, 51(1), 729-774.
- 519
- 520 [22] Iglauer, S., Al-Yaseri, A. Z., Rezaee, R., & Lebedev, M. (2015b). CO<sub>2</sub>  
521 wettability of caprocks: Implications for structural storage capacity and  
522 containment security. *Geophysical Research Letters*, 42(21), 9279-9284.
- 523

- 524 [23] Iglauer, S., Wüiling, W., Pentland, C. H., Al-Mansoori, S. K., & Blunt, M. J.  
525 (2011b). Capillary-trapping capacity of sandstones and sandpacks. *SPE*  
526 *Journal*, 16(04), 778-783.  
527
- 528 [24] Iglauer, S., Fernø, M. A., Shearing, P., & Blunt, M. J. (2012a). Comparison of  
529 residual oil cluster size distribution, morphology and saturation in oil-wet and  
530 water-wet sandstone. *Journal of Colloid and Interface Science*, 375(1), 187-  
531 192.  
532
- 533 [25] Juanes, R., Spiteri, E. J., Orr, F. M., & Blunt, M. J. (2006). Impact of relative  
534 permeability hysteresis on geological CO<sub>2</sub> storage. *Water Resources Research*,  
535 42(12).  
536
- 537 [26] Iglauer, S. (2011c). Dissolution trapping of carbon dioxide in reservoir  
538 formation brine-a carbon storage mechanism. *INTECH Open Access*  
539 *Publisher*.  
540
- 541 [27] Lindeberg, E., Wessel-Berg, D. (1997). Vertical convection in an aquifer  
542 column under a gas cap of CO<sub>2</sub>, *Energy Conversion Management*, 38, 1, 229-  
543 234.  
544
- 545 [28] Gaus, I. (2010). Role and impact of CO<sub>2</sub>-rock interactions during CO<sub>2</sub> storage  
546 in sedimentary rocks. *International Journal of Greenhouse Gas Control*, 4(1),  
547 73-89.  
548
- 549 [29] Golding, S. D., Uysal, I. T., Boreham, C. J., Kirste, D., Baublys, K. A., &  
550 Esterle, J. S. (2011). Adsorption and mineral trapping dominate CO<sub>2</sub> storage in  
551 coal systems. *Energy Procedia*, 4, 3131-3138.  
552
- 553 [30] White, C. M., Smith, D. H., Jones, K. L., Goodman, A. L., Jikich, S. A.,  
554 LaCount, R. B., ... & Schroeder, K. T. (2005). Sequestration of carbon dioxide  
555 in coal with enhanced coalbed methane recovery a review. *Energy & Fuels*,  
556 19(3), 659-724.  
557

- 558 [31] Busch, A., Gensterblum, Y., & Krooss, B. M. (2003). Methane and CO<sub>2</sub>  
559 sorption and desorption measurements on dry Argonne premium coals: pure  
560 components and mixtures. *International Journal of Coal Geology*, 55(2), 205-  
561 224.
- 562  
563 [32] Clarkson, C. R., & Bustin, R. M. (2000). Binary gas adsorption/desorption  
564 isotherms: effect of moisture and coal composition upon carbon dioxide  
565 selectivity over methane. *International Journal of Coal Geology*, 42(4), 241-  
566 271.
- 567  
568 [33] Krooss, B. M., Van Bergen, F., Gensterblum, Y., Siemons, N., Pagnier, H. J.  
569 M., & David, P. (2002). High-pressure methane and carbon dioxide adsorption  
570 on dry and moisture-equilibrated Pennsylvanian coals. *International Journal*  
571 *of Coal Geology*, 51(2), 69-92.
- 572  
573 [34] Saghafi, A., Javanmard, H., & Pinetown, K. (2014). Study of coal gas  
574 wettability for CO<sub>2</sub> storage and CH<sub>4</sub> recovery. *Geofluids*, 14(3), 310-325.
- 575  
576 [35] Kaveh, N. S., Wolf, K. H., Ashrafizadeh, S. N., & Rudolph, E. S. J. (2012).  
577 Effect of coal petrology and pressure on wetting properties of wet coal for  
578 CO<sub>2</sub> and flue gas storage. *International Journal of Greenhouse Gas*  
579 *Control*, 11, S91-S101.
- 580  
581 [36] Sakurovs, R., & Lavrencic, S. (2011). Contact angles in CO<sub>2</sub>-water-coal  
582 systems at elevated pressures. *International Journal of Coal Geology*, 87(1),  
583 26-32.
- 584  
585 [37] Siemons, N., Bruining, H., Castelijns, H., & Wolf, K. H. (2006). Pressure  
586 dependence of the contact angle in a CO<sub>2</sub>-H<sub>2</sub>O-coal system. *Journal of*  
587 *Colloid and Interface Science*, 297(2), 755-761.
- 588  
589 [38] Crawford, R. J., Guy, D. W., & Mainwaring, D. E. (1994). The influence of  
590 coal rank and mineral matter content on contact angle hysteresis. *Fuel*, 73(5),  
591 742-746.

592  
593  
594  
595  
596  
597  
598  
599  
600  
601  
602  
603  
604  
605  
606  
607  
608  
609  
610  
611  
612  
613  
614  
615  
616  
617  
618  
619  
620  
621  
622  
623  
624

- [39] Aplan, F. F. (1993). Coal properties dictate coal flotation strategies. *Mining Engineering*, 45(1), 83-96.
- [40] Gutierrez-Rodriguez, J. A., Purcell, R. J., & Aplan, F. F. (1984). Estimating the hydrophobicity of coal. *Colloids and Surfaces*, 12, 1-25.
- [41] Keller, D. V. (1987). The contact angle of water on coal. *Colloids and surfaces*, 22(1), 21-35.
- [42] Chi, S. M., Morsi, B. I., Klinzing, G. E., & Chiang, S. H. (1988). Study of interfacial properties in the liquid carbon dioxide-water-coal system. *Energy & Fuels*, 2(2), 141-145.
- [43] Kaveh, N. S., Rudolph, E. S. J., Wolf, K. H. A., & Ashrafizadeh, S. N. (2011). Wettability determination by contact angle measurements: hvBb coal–water system with injection of synthetic flue gas and CO<sub>2</sub>. *Journal of Colloid and Interface Science*, 364(1), 237-247.
- [44] Marmur, A. (2006). Soft contact: measurement and interpretation of contact angles. *Soft Matter*, 2(1), 12-17.
- [45] Letellier, P., Mayaffre, A., & Turmine, M. (2007). Drop size effect on contact angle explained by nonextensive thermodynamics. Young's equation revisited. *Journal of Colloid and Interface Science*, 314(2), 604-614.
- [46] Averitt, P. (1975). Coal resources of the United States. January, 1, 1974.
- [47] Bustin, R. M., Barnes, M. A., & Barnes, W. C. (1985). Diagenesis 10. Quantification and modelling of organic diagenesis. *Geoscience Canada*, 12(1).

- 625 [48] Lander, L. M., Siewierski, L. M., Brittain, W. J., & Vogler, E. A. (1993). A  
626 systematic comparison of contact angle methods. *Langmuir*, 9(8), 2237-2239.  
627
- 628 [49] Iglauer, S., Salamah, A., Sarmadivaleh, M., Liu, K., & Phan, C. (2014).  
629 Contamination of silica surfaces: Impact on water–CO<sub>2</sub>–quartz and glass  
630 contact angle measurements. *International Journal of Greenhouse Gas  
631 Control*, 22, 325-328.  
632
- 633 [50] Al-Yaseri, A. Z., Lebedev, M., Barifcani, A., & Iglauer, S. (2016). Receding  
634 and advancing (CO<sub>2</sub>+ brine+ quartz) contact angles as a function of pressure,  
635 temperature, surface roughness, salt type and salinity. *The Journal of  
636 Chemical Thermodynamics*, 93, 416-423.  
637
- 638 [51] Sarmadivaleh, M., Al-Yaseri, A. Z., & Iglauer, S. (2015). Influence of  
639 temperature and pressure on quartz–water–CO<sub>2</sub> contact angle and CO<sub>2</sub>–water  
640 interfacial tension. *Journal of Colloid and Interface Science*, 441, 59-64.  
641
- 642 [52] Ibrahim, A. F., & Nasr-El-Din, H. A. (2015, June). Effects of Water Salinity,  
643 CO<sub>2</sub> Solubility, and Gas Composition on Coal Wettability. In *EUROPEC  
644 2015*. Society of Petroleum Engineers.  
645
- 646 [53] Arif, M., Al-Yaseri, A. Z., Barifcani, A., Lebedev, M., & Iglauer, S. (2016).  
647 Impact of pressure and temperature on CO<sub>2</sub>–brine–mica contact angles and  
648 CO<sub>2</sub>–brine interfacial tension: Implications for carbon geo-sequestration.  
649 *Journal of Colloid and Interface Science*, 462, 208-215.  
650
- 651 [54] Broseta, D., Tonnet, N., & Shah, V. (2012). Are rocks still water-wet in the  
652 presence of dense CO<sub>2</sub> or H<sub>2</sub>S? *Geofluids*, 12(4), 280-294.  
653
- 654 [55] Chiquet, P., Broseta, D., & Thibeau, S. (2007). Wettability alteration of  
655 caprock minerals by carbon dioxide. *Geofluids*, 7(2), 112-122.  
656



- 657 [56] Farokhpoor, R., Bjørkvik, B. J., Lindeberg, E., & Torsæter, O. (2013).  
658 Wettability behaviour of CO<sub>2</sub> at storage conditions. *International Journal of*  
659 *Greenhouse Gas Control*, 12, 18-25.  
660
- 661 [57] Saraji, S., Piri, M., & Goual, L. (2014). The effects of SO<sub>2</sub> contamination,  
662 brine salinity, pressure, and temperature on dynamic contact angles and  
663 interfacial tension of supercritical CO<sub>2</sub>/brine/quartz systems. *International*  
664 *Journal of Greenhouse Gas Control*, 28, 147-155.  
665
- 666 [58] Iglauer, S., Mathew, M. S., & Bresme, F. (2012b). Molecular dynamics  
667 computations of brine–CO<sub>2</sub> interfacial tensions and brine–CO<sub>2</sub>–quartz contact  
668 angles and their effects on structural and residual trapping mechanisms in  
669 carbon geo-sequestration. *Journal of Colloid and Interface Science*, 386(1),  
670 405-414.  
671
- 672 [59] Bae, J. S., & Bhatia, S. K. (2006). High-pressure adsorption of methane and  
673 carbon dioxide on coal. *Energy & Fuels*, 20(6), 2599-2607.  
674
- 675 [60] Fitzgerald, J. E., Pan, Z., Sudibandriyo, M., Robinson Jr, R. L., Gasem, K. A.  
676 M., & Reeves, S. (2005). Adsorption of methane, nitrogen, carbon dioxide and  
677 their mixtures on wet Tiffany coal. *Fuel*, 84(18), 2351-2363.  
678
- 679 [61] Li, D., Liu, Q., Weniger, P., Gensterblum, Y., Busch, A., & Krooss, B. M.  
680 (2010). High-pressure sorption isotherms and sorption kinetics of CH<sub>4</sub> and  
681 CO<sub>2</sub> on coals. *Fuel*, 89(3), 569-580.  
682
- 683 [62] Siemons, N., & Busch, A. (2007). Measurement and interpretation of  
684 supercritical CO<sub>2</sub> sorption on various coals. *International Journal of Coal*  
685 *Geology*, 69(4), 229-242.  
686
- 687 [63] Karacan, C. O., & Okandan, E. (2001). Adsorption and gas transport in coal  
688 microstructure: investigation and evaluation by quantitative X-ray CT  
689 imaging. *Fuel*, 80(4), 509-520.  
690

- 691 [64] Hol, S., & Spiers, C. J. (2012). Competition between adsorption-induced  
692 swelling and elastic compression of coal at CO<sub>2</sub> pressures up to 100MPa.  
693 *Journal of the Mechanics and Physics of Solids*, 60(11), 1862-1882.  
694
- 695 [65] Reucroft, P. J., & Sethuraman, A. R. (1987). Effect of pressure on carbon  
696 dioxide induced coal swelling. *Energy & Fuels*, 1(1), 72-75.  
697
- 698 [66] Wang, Q., Zhang, D., Wang, H., Jiang, W., Wu, X., Yang, J., & Huo, P.  
699 (2015). Influence of CO<sub>2</sub> Exposure on High-pressure Methane and CO<sub>2</sub>  
700 Adsorption on Various Rank Coals: Implications for CO<sub>2</sub> Sequestration in  
701 Coal Seams. *Energy & Fuels*.  
702
- 703 [67] Zhou, F., Hussain, F., & Cinar, Y. (2013). Injecting pure N<sub>2</sub> and CO<sub>2</sub> to coal  
704 for enhanced coalbed methane: experimental observations and numerical  
705 simulation. *International Journal of Coal Geology*, 116, 53-62  
706
- 707 [68] Li, X., Boek, E., Maitland, G. C., & Trusler, J. M. (2012). Interfacial Tension  
708 of (Brines+ CO<sub>2</sub>): (0.864 NaCl+ 0.136 KCl) at Temperatures between (298  
709 and 448) K, Pressures between (2 and 50) MPa, and Total Molalities of (1 to  
710 5) mol· kg<sup>-1</sup>. *Journal of Chemical & Engineering Data*, 57(4), 1078-1088.  
711
- 712 [69] Bustin, R. M., & Clarkson, C. R. (1998). Geological controls on coalbed  
713 methane reservoir capacity and gas content. *International Journal of Coal  
714 Geology*, 38(1), 3-26.  
715
- 716 [70] Levy, J. H., Day, S. J., & Killingley, J. S. (1997). Methane capacities of  
717 Bowen Basin coals related to coal properties. *Fuel*, 76(9), 813-819.  
718
- 719 [71] Perera, M. S. A., Ranjith, P. G., Choi, S. K., Bouazza, A., Kodikara, J., &  
720 Airey, D. (2011). A review of coal properties pertinent to carbon dioxide  
721 sequestration in coal seams: with special reference to Victorian brown coals.  
722 *Environmental Earth Sciences*, 64(1), 223-235.  
723

- 724 [72] Perera, M. S. A., Ranjith, P. G., Choi, S. K., Airey, D., & Weniger, P. (2012).  
725 Estimation of gas adsorption capacity in coal: a review and an analytical  
726 study. *International Journal of Coal Preparation and Utilization*, 32(1), 25-  
727 55.
- 728
- 729 [73] Sakurovs, R., Day, S., Weir, S., & Duffy, G. (2007). Application of a modified  
730 Dubinin-Radushkevich equation to adsorption of gases by coals under  
731 supercritical conditions. *Energy & Fuels*, 21(2), 992-997.
- 732
- 733 [74] Zhang, L., Aziz, N. I., Ren, T., & Wang, Z. (2011). Influence of temperature  
734 on the gas content of coal and sorption modelling.
- 735
- 736 [75] Mastalerz, M., Gluskoter, H., & Rupp, J. (2004). Carbon dioxide and methane  
737 sorption in high volatile bituminous coals from Indiana, USA. *International*  
738 *Journal of Coal Geology*, 60(1), 43-55.
- 739
- 740 [76] Durucan, S., Ahsan, M., Shi, J. Q., Syed, A., & Korre, A. (2014). Two phase  
741 relative permeabilities for gas and water in selected European coals. *Fuel*, 134,  
742 226-236.
- 743
- 744 [77] Zhang, J., Feng, Q., Zhang, X., Wen, S., & Zhai, Y. (2015). Relative  
745 permeability of coal: a review. *Transport in Porous Media*, 106(3), 563-594.
- 746
- 747 [78] Hamawand, I., Yusaf, T., & Hamawand, S. G. (2013). Coal seam gas and  
748 associated water: a review paper. *Renewable and Sustainable Energy Reviews*,  
749 22, 550-560.
- 750
- 751 [79] Busch, A., Gensterblum, Y., Krooss, B. M., & Littke, R. (2004). Methane and  
752 carbon dioxide adsorption–diffusion experiments on coal: upscaling and  
753 modeling. *International Journal of Coal Geology*, 60(2), 151-168.
- 754
- 755 [80] Pini, R., Ottiger, S., Storti, G., & Mazzotti, M. (2010). Prediction of  
756 competitive adsorption on coal by a lattice DFT model. *Adsorption*, 16(1-2),  
757 37-46.

758  
759  
760  
761  
762  
763  
764  
765

[81] Reeves, S., Gonzalez, R., Gasem, K. A., Fitzgerald, J. E., Pan, Z., Sudibandriyo, M., & Robinson Jr, R. L. (2005, May). Measurement and prediction of single- and multi-component methane, carbon dioxide and nitrogen isotherms for US coals. In 2005 *International Coalbed Methane Symposium*, Paper (Vol. 527, pp. 16-20).